Spectral and thermal dependence of phase coherent photorefractivity in ZnSe quantum wells

H. P. Wagner, S. Tripathy, P. Bajracharya, and H.-P. Tranitz*
Department of Physics, University of Cincinnati, Cincinnati, Ohio 45221-0011, USA
(Received 15 September 2005; published 17 February 2006)

We investigate the spectral and thermal dependence of an exciton resonant all-optical and phase coherent photorefractive effect in a ZnSe single quantum well by four-wave mixing using 90 fs pulses. The observed phase coherence is attributed to an exciton-induced formation of an electron grating within the quantum well. The diffracted signal exhibits an exponential decay that is equal to the exciton dephasing rate and it shows a pronounced suppression at the temporal overlap of incident pulses. With decreasing photon energy the diffracted signal traces reveal faster decay and the exciton transition is shifted towards lower energies indicating an increasing electron concentration within the quantum well. In temperature dependent measurements we observe a filling of the signal dip at pulse overlap and a transition from the photorefractive effect to a $\chi^{(3)}$ four-wave-mixing process below 35 K. Additional experiments using a cw pump laser are consistent with the proposed mechanism of the observed photorefractive effect. The phase coherent photorefractive signal is reproduced by a phenomenological model that is based on the optical Bloch equations for a five-level system.

DOI: 10.1103/PhysRevB.73.085318 PACS number(s): 78.67.De, 71.55.Gs, 71.35.−y, 42.50.Md

I. INTRODUCTION

The large excitonic nonlinearities of multiple quantum well (QW) structures have been used in the last decade to fabricate photorefractive (PR) devices that open new possibilities for optical data storage and optical computation.[1–20] In particular PR multiple QWs enable much shorter times to write or erase a grating compared to bulk PR materials and they show strong Franz-Keldysh[3,4,10,13,17,18] and quantum confined Stark effect (QCSE)[11,12,14–16,19] when transverse or longitudinal external fields are applied with respect to the QW growth direction. Because of their high sensitivity and fast response two dimensional optical imaging devices[20] as well as other applications, e.g., femtosecond pulse shaping,[21] laser based ultrasound detection[22] and three-dimensional depth resolved holographic imaging[23] have been demonstrated recently. So far mainly III-V based photorefractive multiple QWs have been studied where the external fields have been provided by electrical contacts on top of the devices. Very few investigations have been reported on II-VI QWs (Refs. 2, 8, and 24) which are supposed to have higher optical nonlinearities than III-V QWs.[25] There are also not many investigations on all-optical PR multiple QW structures[6–8] that operate without electrical contacts thus avoiding the elaborate sample processing and enhancing the integrability into miniaturized devices for optical information processing. To date there are no PR devices that use the coherence of excitons to conserve the phase and polarization information of incident light fields. Such all-optical phase coherent photorefractive (PCP) quantum well structures[26] would strongly impact research areas such as optical data storage and optical computation.

In this paper we report on the spectral and thermal dependence of a novel all-optical PCP effect in a $ZnSe/Zn_{0.94}Mg_{0.06}Se$ single QW using ultrashort 90 fs laser pulses in a four-wave-mixing configuration. As described recently[26] the PCP effect is attributed to the formation of a long living electron grating that is generated in a multistep process: First excess electrons, as evidenced by previous studies,[27,28] are optically excited in the GaAs substrate and subsequently captured in the QW. Second, an exciton grating is generated by the interference of coherent exciton polarizations created by pulses $\mathbf{k}_1$ and $\mathbf{k}_2$. Third, the QW electrons are redistributed by the exciton grating into regions of low exciton density due to Coulomb interaction and Pauli blocking. After the exciton lifetime ($\sim$100 ps) the exciton density grating vanishes by recombination, while the long living (>10 μs) π-shifted electron grating that is stabilized by localized holes at the ZnSe/GaAs interface remains in the QW. The electron grating supplies longitudinal space charge fields between the QW and localized interface charges as well as excitation induced dephasing (EID).[29] Both effects are responsible for the occurrence of a PCP effect. Correspondingly, this novel effect combines the phase coherence of excitons with strong electro-optic effects caused by the electron grating within the QW. The additional degree of phase coherence in these QW structures may open new design possibilities for data storage and computational applications. Spectral and temperature-dependent studies of this phase coherent photorefractivity further elucidate the coherent formation of the electron grating. The experimentally observed PR signal is successfully reproduced by a phenomenological model that is based on the optical Bloch equation for a five-level system.

II. EXPERIMENTAL DETAILS

The investigated ZnSe single QW was pseudomorphically grown on (001) oriented GaAs substrate by molecular beam epitaxy. The sample consists of a 10-nm-wide ZnSe QW sandwiched between two 30-nm $Zn_{0.94}Mg_{0.06}Se$ barriers, with a 20-nm-thick ZnSe buffer layer between the barrier and the GaAs substrate. A detailed description of the growth and sample characterization is given in Ref. 30. A frequency doubled mode locked Ti-sapphire laser providing ultrashort pulses of a spectral width of 22 meV at a repetition rate of 80 MHz was used to excite the sample. The temporal width

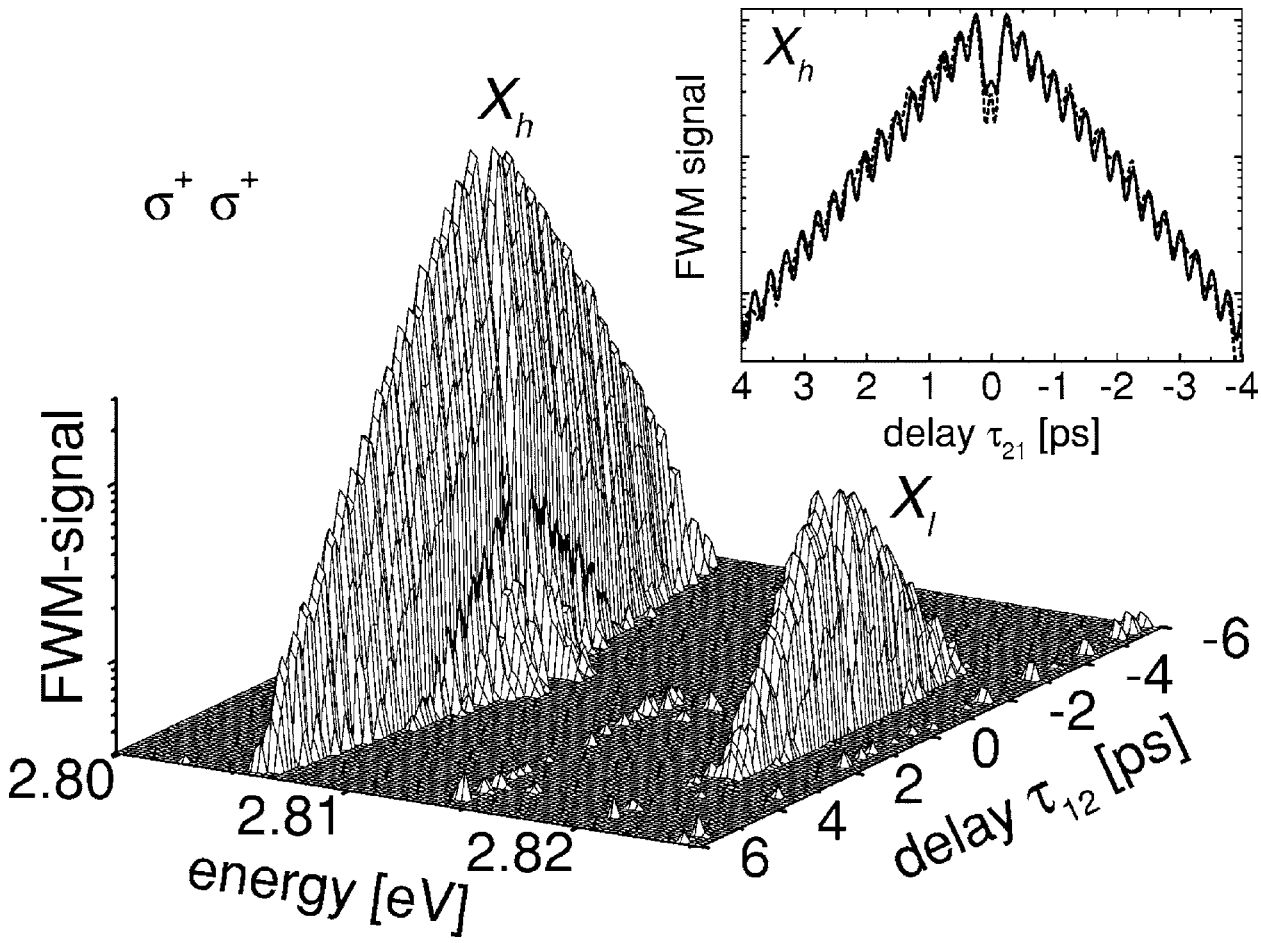

FIG. 1. Spectrally resolved PR signal into $2\mathbf{k}_2-\mathbf{k}_1$ direction as a function of delay τ_{12} recorded at a lattice temperature of 55 K. The total intensity of the cocircular polarized pulses is 20 kW cm^{-2}. The inset shows the calculated trace at the X_h heavy-hole exciton transition as described in the text (full line) in comparison to the experimentally observed trace (dashed line).

of the frequency doubled pulses was determined to be 90±5 fs using an autocorrelation technique that is based on two-photon-absorption in a SiC photodiode. Two- and three-beam four-wave-mixing (FWM) experiments involving pulses $\mathbf{k}_1$, $\mathbf{k}_2$, and $\mathbf{k}_3$ with arrival times t_1, t_2, and t_3, respectively, have been performed in back scattering geometry with the sample mounted in a closed cycle cryostat at temperatures between 25 and 65 K. In the three-beam FWM experiments the delay time between $\mathbf{k}_1$ and $\mathbf{k}_3$ was kept to 10 ps ($\tau_{13}=t_3-t_1\approx 10$ ps) while the time delay $\tau_{12}=t_2-t_1$ was varied between pulses $\mathbf{k}_1$ and $\mathbf{k}_2$. The zero delay between different pulses has been determined by the contrast of the interference pattern appearing on the sample surface during the temporal overlap of the pulses. The $1/e^2$ focus diameter of the laser pulses on the sample was 100 μm. The time integrated and spectrally resolved four wave mixing signal was detected in direction $2\mathbf{k}_2-\mathbf{k}_1$ and $\mathbf{k}_3+\mathbf{k}_2-\mathbf{k}_1$, respectively, by a combination of a spectrometer and an optical multichannel analyzer. The two-beam experiments have been performed in co-circular polarization configuration ($\sigma^+\sigma^+$) of incident pulses $\mathbf{k}_1$ and $\mathbf{k}_2$. In three-beam experiments we used circular configurations ($\sigma^+\sigma^+\sigma^+$), ($\sigma^-\sigma^-\sigma^+$), and ($\sigma^+\sigma^-\sigma^+$), where the first, second and third symbol in the parentheses indicates the circular polarization of pulse $\mathbf{k}_1$, $\mathbf{k}_2$, and $\mathbf{k}_3$, respectively.

III. EXPERIMENTAL RESULTS AND DISCUSSION

A. Exciton resonant PCP effect

Figure 1 shows the spectrally resolved PR signal in $2\mathbf{k}_2-\mathbf{k}_1$ direction as a function of delay τ_{12} for ($\sigma^+\sigma^+$) polarized fields at a temperature of 55 K. The center of the 22 meV broad excitation pulse was set to 2.808 eV, in order to avoid continuum contributions and predominantly excite the X_h heavy-hole exciton at 2.806 eV and weakly excite the light-hole X_l exciton transition at 2.821 eV. The total excitation intensity of pulses $\mathbf{k}_1$ and $\mathbf{k}_2$ was 20 kW cm^{-2} in these experiments (corresponding to a total average power of 12 μW). As described in previous investigations[26] the signal slope approaches the value $2\gamma_2$ (with γ_2 being the exciton dephasing rate) for negative ($\tau_{12}<0$) and positive delay times ($\tau_{12}>0$). Furthermore the signal trace reveals a pronounced dip at temporal pulse overlap $\tau_{12}=0$. In addition quantum beats between heavy- and light-hole excitons with a period of $\Delta\tau\approx 280$ fs (corresponding to an energy splitting of $\Delta E_{hl}=h/\Delta\tau\approx 15$ meV) are observed in the PR signal traces.

As mentioned earlier, the PCP effect is attributed to the formation of an electron grating that is induced by an exciton grating. Longitudinal space charge fields within the QW and

the GaAs/ZnSe interface cause a periodic modulation of the optical constants via QCSE that lead to a diffraction of exciton polarization $\mathbf{P}_{\mathbf{k}_2}$ into direction $2\mathbf{k}_2-\mathbf{k}_1$. In addition to this exciton resonant electro-optic effect the spatial modulation of the electron density itself also contributes to a diffracted exciton polarization via EID[29] leading to a spectral diffraction efficiency of $\eta\approx 3\times 10^{-4}$ as described in Ref. 26.

During pulse overlap the excitation density in the GaAs substrate is spatially modulated, giving rise to a second contribution of the electron density grating in the QW, that is in phase with the exciton density grating. Since this pulse overlap contribution is inverted to the earlier described grating (that is created by the redistribution of electrons) the total PR signal is suppressed at $\tau_{12}\approx 0$.

For a quantitative description the PR response obtained in two-pulse configuration is modeled using the optical Bloch equations (OBE) of a five-level system for δ-shaped laser pulses. The five-level model with the ground level $|1\rangle$ initially populated takes into account the nature of σ^+ and $\sigma^- X_h$ excitons (levels $|2\rangle$ and $|3\rangle$) and X_l excitons (levels $|4\rangle$ and $|5\rangle$). After Fourier transformation the diffracted polarization into direction $2\mathbf{k}_2-\mathbf{k}_1$ reads

$$\mathbf{P}_2(\omega,\tau_{12}) \propto [-a_{\mathbf{k}_2-\mathbf{k}_1}(\tau_{12})+b_{\mathbf{k}_2-\mathbf{k}_1}(\tau_{12})] \times\exp(-t_{\mathrm{rep}}/T_g)\sum_{j=2}^{5}\frac{\boldsymbol{\mu}_{j1}(\boldsymbol{\mu}_{j1}\cdot\mathbf{e}_2)}{(\Omega_{j1}-\omega)} \times\exp(i\omega\tau_{12}). \quad (1)$$

Function $a_{\mathbf{k}_2-\mathbf{k}_1}(\tau_{12})$ describes the density of the exciton grating that is responsible for the subsequent formation of an electron grating in regions of low exciton density, given by

$$a_{\mathbf{k}_2-\mathbf{k}_1}(\tau_{12}) = a\theta(-\tau_{12})\sum_{j=2}^{5}(\boldsymbol{\mu}_{j1}\cdot\mathbf{e}_2)(\boldsymbol{\mu}_{j1}^*\cdot\mathbf{e}_1^*)\exp(i\Omega_{j1}\tau_{12}) + a\theta(\tau_{12})\sum_{j=2}^{5}(\boldsymbol{\mu}_{j1}\cdot\mathbf{e}_2)(\boldsymbol{\mu}_{j1}^*\cdot\mathbf{e}_1^*)\exp(i\Omega_{j1}^*\tau_{12}). \quad (2)$$

Unit vectors $\mathbf{e}_1$ and $\mathbf{e}_2$ denote the polarization of σ^+ and σ^- polarized laser pulses $\mathbf{k}_1$ and $\mathbf{k}_2$ with $\boldsymbol{\sigma}^{\pm}=2^{-0.5}(1,\mp i)$ in Jones notation. The optical matrix elements $\boldsymbol{\mu}_{1j}$ are given by $\boldsymbol{\mu}_{12}=\mu_{12}\boldsymbol{\sigma}^+$, $\boldsymbol{\mu}_{15}=\mu_{15}\boldsymbol{\sigma}^+$ and $\boldsymbol{\mu}_{13}=\mu_{13}\boldsymbol{\sigma}^-$, $\boldsymbol{\mu}_{14}=\mu_{14}\boldsymbol{\sigma}^-$ where μ_{1j} accounts for the magnitude of the dipole transitions. Furthermore we have used the abbreviations $\Omega_{j1}=\omega_{j1}-i\gamma_2$ where the ω_{j1} denote the angular frequencies between ground state $|1\rangle$ and the σ^+ ($|2\rangle$, $|4\rangle$) and σ^- ($|3\rangle$, $|5\rangle$) exciton levels, respectively. The empirical parameter a accounts for the efficiency of the PR effect. $t_{\mathrm{rep}}=12.5$ ns is the pulse repetition time. Time constant T_g gives the lifetime of the electron grating that is determined by lateral diffusion and electron escape, considering that polarization $\mathbf{P}_{\mathbf{k}_2}$ is diffracted from the partly decayed "old" $\mathbf{k}_2-\mathbf{k}_1$ grating that was created in previous pulse cycles.

Function $b_{\mathbf{k}_2-\mathbf{k}_1}(\tau_{12})$ in Eq. (1) describes the electron density grating that is created during pulse overlap and is given by

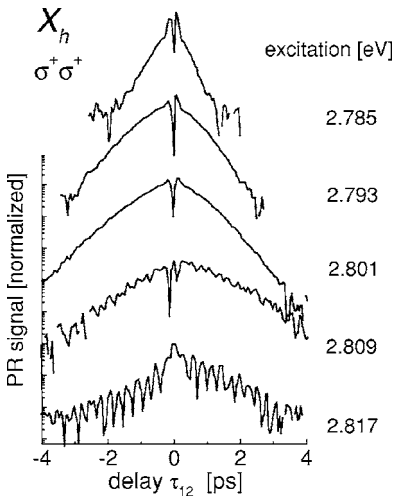

FIG. 2. Traces of the diffracted $2\mathbf{k}_2-\mathbf{k}_1$ PR signal at the X_h heavy-hole exciton transition as a function of delay τ_{12} recorded at a lattice temperature of 55 K and at different excitation energies as labeled. The pulse intensities of cocircular polarized pulses $\mathbf{k}_1$ and $\mathbf{k}_2$ are $I_1=80$, and $I_2=40$ kW cm^{-2}, respectively.

$$b_{\mathbf{k}_2-\mathbf{k}_1}(\tau_{12}) = b\mathbf{e}_2\cdot\mathbf{e}_1^*\exp(i\omega_p\tau_{12})\left(\int E_{\mathbf{k}_2}(t-\tau_{12})E_{\mathbf{k}_1}(t)dt\right). \quad (3)$$

In Eq. (3) the integral gives the field autocorrelation of sech(t) shaped pulses with temporal full width at half maximum (FWHM) of $1.49\Delta t$, where Δt is the measured intensity FWMH of the incident laser pulses. ω_p is the center frequency of the pulse, b is an adjustable parameter in order to obtain optimum agreement with the observed signal at $\tau_{12}\approx 0$. The minus sign in Eq. (1) considers the π shift of this electron grating with respect to the formed exciton grating.

The inset in Fig. 1 displays the numerical calculation at the spectral position of the X_h heavy-hole exciton (solid line). The energetic position of the exciton transition was taken from the experimental spectra, the magnitude of the ground to heavy-hole dipole matrix elements $\mu_{21}=\mu_{31}$ and that of the ground to light-hole exciton dipole matrix elements $\mu_{41}=\mu_{51}$ were set to 1 and 0.57, respectively, according to their relative oscillator strength ratios $\mu_{21}{}^2:\mu_{41}{}^2$ of 3:1 given by their different valence band Bloch functions. In the calculation we further considered the spectral intensity of the pulse at the X_h and X_l transition energy. From the signal trace we evaluated the exciton dephasing time to $T_2=1.55$ ps. For the electron grating lifetime T_g we used 10 μs,[26] for the temporal FWHM of the excitation pulses we applied $\Delta t=90$ fs, and parameter b was adjusted to 0.6. The overall agreement between the model calculations and the experimental data is good.

B. Spectral dependence of the PCP effect

Figure 2 shows the normalized PR signal traces in $2\mathbf{k}_2-\mathbf{k}_1$ direction as a function of delay τ_{12} for $(\sigma^+\sigma^+)$ polarized fields at a temperature of 55 K. The center energy of the excitation pulses was changed from 2.785 to 2.817 eV in

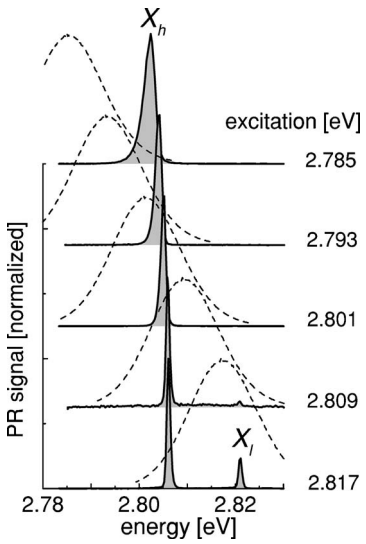

FIG. 3. Spectra of the diffracted $2\mathbf{k}_2-\mathbf{k}_1$ PR signal for positive delay $\tau_{12}>0$ recorded at a lattice temperature of 55 K and at different excitation energies as labeled. The dashed lines show the spectra of the excitation pulses for comparison. The used pulse intensities are the same as in Fig. 2.

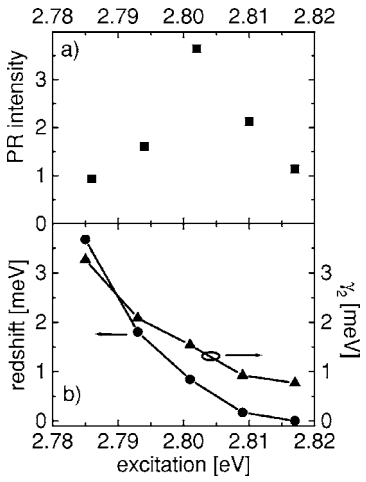

FIG. 4. PR signal intensities (a) and energy shift at $\tau_{12}=500$ fs as well as exciton dephasing rates γ_2 (b) of the X_h exciton transition as a function of the excitation energy.

8 meV steps. In these experiments the excitation intensity of pulses $\mathbf{k}_1$ and of $\mathbf{k}_2$ was set to 80 and 40 kW cm^{-2}, respectively (corresponding to a total average power of 70 μW). While the signal trace excited at 2.809 eV shows a similar behavior as in Fig. 1 the traces at lower excitation energies reveal no X_h-X_l beating and possess higher decay rates. In addition the shape of the PR signals becomes asymmetric with faster decay for $\tau_{12}>0$ and slower decay for $\tau_{12}<0$. In contrast the PR signal excited at highest energy (2.817 eV) shows a lower decay rate for positive delay but a higher rate for negative delay. Furthermore the signal dip starts to disappear at excitation energies above 2.801 eV.

Figure 3 depicts the PR signal spectra at $\tau_{12}=500$ fs obtained at different excitation energies as labeled. In addition the spectra of excitation pulses are given as dashed curves for comparison. While both heavy X_h and light-hole excitons X_l are excited at 2.817 and 2.809 eV all other spectra are dominated by the X_h exciton explaining the lack of quantum beats in the signal traces below 2.809 eV (see Fig. 2). Furthermore the peak position of the heavy-hole exciton X_h is shifted to lower energies when the ZnSe QW is excited below 2.809 eV.

Figure 4(a) represents the relative PR signal intensities for the different excitation energies revealing a maximum signal intensity at an excitation energy of 2.801 eV. Figure 4(b) summarizes the energy shift of the X_h exciton transition and the exciton decay rates as a function of the excitation energy. The observed dependencies clearly indicate that the resonant diffraction is caused both by a periodic modulation of the exciton transition energy, usually expected from QCSE, as well as by a periodic modulation of the exciton dephasing time also known as EID.[29]

According to our assumption that the resonant PCP effect is attributed to an electron grating created by captured QW electrons with density n_e we conclude from Figs. 2–4 that the electron density n_e increases with decreasing excitation energy. The increase of n_e is attributed to an increased transparency of the ZnSe buffer layer (excitation below the band gap) on top of the GaAs substrate as well as to a decreased density of excited QW excitons. The lower exciton density leads to reduced electron escape rate due to Auger processes that are caused by the recombination of excitons. The increased captured electron density leads to an enhanced exciton-electron scattering that increases the exciton dephasing rate γ_2 according to

$$\gamma_2(n_X,n_e,T)=\gamma_2(n_X,T)+\beta_{Xe}n_e \tag{4}$$

with β_{Xe} being the exciton-electron scattering parameter and n_e being the electron density. The expression

$$\gamma_2(n_X,T)=\gamma_{20}+\beta_{\mathrm{ac}}T+\frac{\beta_{\mathrm{LO}}}{\exp[E_{\mathrm{LO}}/(k_BT)]-1}+\beta_{XX}n_X \tag{5}$$

describes the exciton dephasing rate extrapolated to zero electron density with background dephasing rate γ_{20}, acoustic and LO-phonon scattering parameters β_{ac} and β_{LO}, respectively, and T being the lattice temperature. Furthermore β_{XX} is the exciton-exciton scattering parameter and n_X is the exciton density. To calculate the static space charge fields we estimated the electron density n_e using an acoustic phonon scattering parameter $\beta_{\mathrm{ac}}=7.6\times10^8$ s^{-1} K^{-1},[31] a LO-phonon scattering parameter $\beta_{\mathrm{LO}}=3.8\times10^{13}$ s^{-1},[31] the LO-phonon energy $E_{\mathrm{LO}}=31.6$ meV, and an exciton-exciton scattering parameter of $\beta_{XX}=22$ s^{-1} cm^2.[32] From earlier investigations[33] we estimated an exciton density of $n_X\approx1.5\times10^9$ cm^{-2} at 80 kW cm^{-2} pulse intensity. Recently performed intensity dependent FWM measurements on a similar quantum well using 30 fs pulses[34] reveal an exciton-electron-hole pair scattering parameter of $\beta_{X-eh}\approx70\pm20$ s^{-1} cm^2. If we assume that the scattering due to holes is significantly smaller than due to electrons[35] and also assume a background dephasing rate of $\gamma_{20}\approx0$ we estimate an (upper limit) electron density ranging from $n_e\approx0.7\times10^{10}$ cm^{-2} at an excitation energy of 2.817 eV to $n_e\approx2.8\times10^{10}$ cm^{-2} at excitation 2.785 eV.

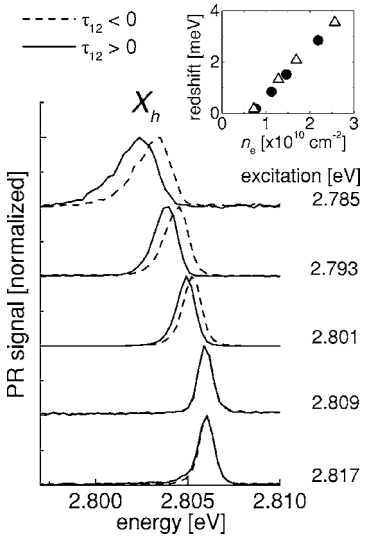

FIG. 5. Spectra of the diffracted $2\mathbf{k}_2-\mathbf{k}_1$ PR signal for positive $\tau_{12}>0$ (solid line) and negative delay $\tau_{12}<0$ (dashed line) recorded at a lattice temperature of 55 K and at different excitation energies as labeled. The inset shows the obtained redshift of the X_h heavy-hole exciton transition as a function of the captured electron density n_e evaluated from Eq. (4). The used pulse intensities are the same as in Fig. 2.

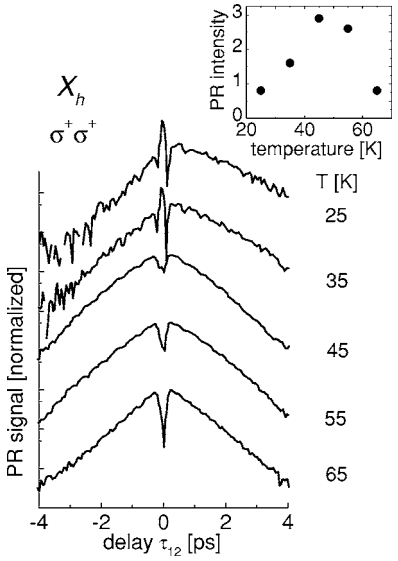

FIG. 6. Traces of the diffracted $2\mathbf{k}_2-\mathbf{k}_1$ PR signal at the X_h heavy-hole exciton transition as a function of delay τ_{12} recorded at excitation energy 2.808 eV and at different lattice temperatures as labeled. The cocircular polarized pulse intensities are $I_1=40$ and $I_2=30$ kW cm^{-2}, respectively. The inset shows the PR signal intensity obtained at $\tau_{12}=500$ fs as a function of temperature.

The increased electron density leads to an increasing electric field E between quantum well electrons and positive charges at the barrier/substrate interface according to $E=\sigma/\varepsilon\varepsilon_0$ with surface charge density $\sigma=n_e e$, e being the electron charge and static dielectric constant $\varepsilon=9$. The maximum E field between the quantum well surface that is adjacent to the barrier substrate interface calculates to $E\approx 6\times 10^3$ V cm^{-1}. Such fields lead to a noticeable tilt of the $Zn_{0.94}Mg_{0.06}Se$ barrier (with $\sim$20 meV conduction band offset[30]) and the ZnSe buffer layer band alignments hence reducing the effective thickness of the barrier that decreases the electron and hole confinement energies due to increased penetration of the wavefunctions into the barrier. The reduction of confinement energies explains the observed redshift of the X_h exciton transition with increasing density n_e.

Figure 5 shows detailed PR spectra of the X_h signal for positive (solid lines) and negative (dashed lines) pulse delay. The inset in Fig. 5 illustrates the observed redshift of the X_h exciton PR signal as a function of the electron density n_e derived from Eq. (4). Since the intensity of pulse $\mathbf{k}_1$ is by a factor of 2 higher than that of pulse $\mathbf{k}_2$ the electron densitiy n_e differs for positive and negative delay leading to a stronger redshift of the X_h PCP signal for $\tau_{12}>0$. Because the field lines start in the quantum well rather than they pass the QW the redshift of the exciton transition versus n_e does not show a quadratic dependence as expected from the QCSE. In addition, as mentioned earlier, EID also efficiently contributes to the observed coherent PR diffraction.

At excitation energies higher than 2.809 eV the reduced transparency of the ZnSe QW and of the ZnSe buffer as well as an increased exciton density n_X lower the captured electron density n_e leading to a decrease of the PR efficiency. Hence the otherwise weak $\chi^{(3)}$ FWM signal process becomes the dominant contribution in the observed signal also explaining the filling of the signal dip at $\tau_{12}\approx 0$ and the faster decay for negative delay compared to $\tau_{12}>0$.[33]

C. Temperature dependence of the PCP effect

Figure 6 shows the PR signal at pulse intensities of 40 and 30 kW cm^{-2} for $\mathbf{k}_1$ and $\mathbf{k}_2$, respectively. The experiments were performed at a pulse energy of 2.806 eV and at temperatures ranging from 25 to 65 K in 10 K steps. The inset of Fig. 6 shows the PR signal intensity as a function of temperature obtained at pulse delay $\tau_{12}=500$ fs. With decreasing temperature the signal dip at $\tau_{12}\approx 0$ is vanishing and the PCP signal intensity significantly decreases below 45 K. The PCP signal finally transforms to a $\chi^{(3)}$ FWM signal below 25 K revealing the well known feature of a twice as fast signal decay for $\tau_{12}<0$ than for $\tau_{12}>0$, for a signal dominated by EID.[29] The observed behavior at lower temperatures is attributed to a reduced mobility of positive charges at the ZnSe/GaAs interface by localization. This effect hinders the redistribution of holes and hence the stabilization of the electron grating within the QW which leads to a decreased PR efficiency. Correspondingly, the $\chi^{(3)}$ FWM signal becomes more important at low temperatures. Furthermore at $\tau_{12}\approx 0$ an electron grating is generated within the QW by the $\mathbf{k}_1$ and $\mathbf{k}_2$ pulse interference within the GaAs substrate that causes an exciton resonant PCP signal in addition to the to the $\chi^{(3)}$ signal explaining the filling of the dip at temporal pulse overlap. Above 55 K the PR signal intensity significantly decreases which is attributed to a thermally activated tunneling of QW electrons back to the GaAs substrate which reduces the lifetime of the induced QW electron grating. According to these experiments there is an optimum

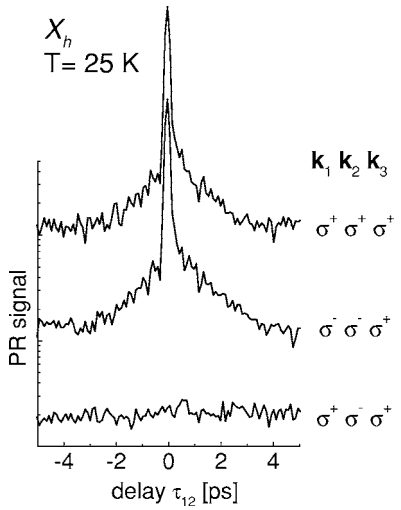

FIG. 7. Traces of the diffracted $\mathbf{k}_3+\mathbf{k}_2-\mathbf{k}_1$ PR signal at the X_h heavy-hole exciton transition for polarization configurations $(\sigma^+\sigma^+\sigma^+)$, $(\sigma^-\sigma^-\sigma^+)$, and $(\sigma^+\sigma^-\sigma^+)$ as a function of delay τ_{12} recorded at a lattice temperature of 25 K. The delay time between $\mathbf{k}_1$ and $\mathbf{k}_3$ was kept fixed to 10 ps. The intensities of pulses $\mathbf{k}_1$, $\mathbf{k}_2$, and $\mathbf{k}_3$ were $I_1=34$, $I_2=24$, and $I_3=60$ kW cm^{-2}, respectively.

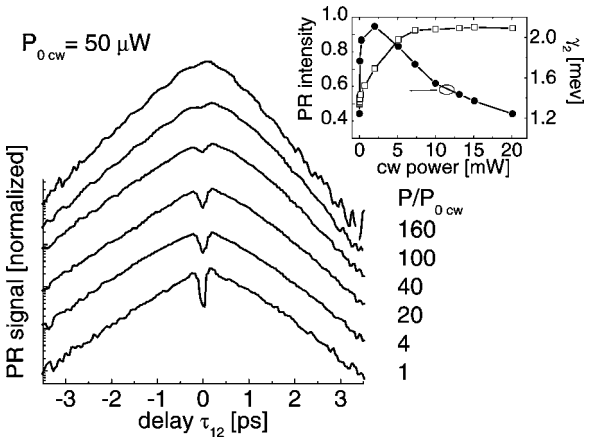

FIG. 8. Traces of the diffracted $2\mathbf{k}_2-\mathbf{k}_1$ PR signal at the X_h exciton transition for polarization configurations $(\sigma^+\sigma^+)$ recorded at 55 K for different spatially uniform cw laser illumination of the GaAs substrate at 637 nm (1.93 eV). The increasing intensity ratio is given with respect to a reference power of $P_0=50$ μW. The inset shows the exciton dephasing rate γ_2 (open squares) as well as the observed signal intensity at $\tau_{12}=500$ fs (full circles) as a function of the cw laser power.

(sample dependent) temperature balancing the hole mobility and the thermal activation of electrons both being responsible for the PCP efficiency.

The PR nature of the signal spike at $\tau_{12}\approx 0$ at temperatures below 35 K is confirmed by three-pulse experiments which were performed in a similar way as described in Ref. 26. The circular polarized pulses possesses intensities $I_1=34$, $I_2=24$, and $I_3=60$ kW cm^{-2} (corresponding to an average pulse power of $P_1=20$, $P_2=14$, and $P_3=36$ μW), respectively. The delay time between $\mathbf{k}_1$ and $\mathbf{k}_3$ was kept fixed to $\tau_{13}=t_3-t_1\approx 10$ ps therefore excluding coherent interactions of pulse $\mathbf{k}_3$ with pulses $\mathbf{k}_1$ and $\mathbf{k}_2$. The delay between pulses $\mathbf{k}_2$ and $\mathbf{k}_1$ was varied where a positive delay $(\tau_{12}=t_2-t_1>0)$ refers to the case where $\mathbf{k}_2$ arrives last whereas a negative delay $(\tau_{12}<0)$ refers to pulse $\mathbf{k}_2$ arriving first. The $\mathbf{k}_3+\mathbf{k}_2-\mathbf{k}_1$ signal response at 25 K at the energetic position of the X_h transition for configuration $(\sigma^+\sigma^+\sigma^+)$, $(\sigma^-\sigma^-\sigma^+)$, and $(\sigma^+\sigma^-\sigma^+)$ are displayed in Fig. 7 as a function of delay time τ_{12}. In $(\sigma^+\sigma^+\sigma^+)$ and $(\sigma^-\sigma^-\sigma^+)$ configuration we observe a pronounced PR signal peak at $\tau_{12}\approx 0$. As expected the PR signal vanishes in $(\sigma^+\sigma^-\sigma^+)$ since $\mathbf{k}_1$ and $\mathbf{k}_2$ have orthogonal polarized fields that cannot produce an electron grating.

D. PCP effect with cw pump laser

Finally, we performed two-beam experiments where carriers in the GaAs substrate are generated by cw and spatially uniform illumination at a wavelength of 637 nm (~1.93 eV). The focus diameter of the cw beam at the sample surface was ~1 mm. The result of the experiments performed at pulse intensities $I_1=I_2=10$ kW cm^{-2} and at 55 K is shown in Fig. 8. With increasing cw laser intensity (reference power $P_0=50$ μW) the exciton dephasing rate γ_2 increases (see inset of Fig. 8) due to an increased electron density n_e that enhances the exciton-electron scattering rate within the QW. Above a cw power level of 7.5 mW the dephasing rate γ_2 saturates which is attributed to a saturating equilibrium density n_e. Furthermore the signal dip at $\tau_{12}\approx 0$ is vanishing. This is a consequence of the reduced contribution of the intensity grating at pulse overlap to the total excitation intensity. The measurements also demonstrate that the PCP efficiency can be enhanced at low cw intensity due to an increased electron density in the QW (see inset of Fig. 8). At higher cw intensities, however, the electron density modulation is significantly reduced due to the continuous and spatially uniform excitation of electrons into the QW. The experiments with cw pump are consistent with the proposed mechanism of the observed PCP due to a coherent exciton diffraction in the quantum well.

IV. SUMMARY

In conclusion we have studied the spectral and thermal dependence of an exciton resonant and phase coherent photorefractive (PCP) effect in a ZnSe single QW. The investigations were performed in two- and three-pulse configuration using 90 fs pulses. At 55 K and equal $\mathbf{k}_1$ and $\mathbf{k}_2$ excitation intensities at 2.808 eV the PCP signal traces show equal decay rates for positive and negative delay and a pronounced signal depression at the temporal overlap of the incident pulses at $\tau_{12}\approx 0$. The experimental results are reproduced by a phenomenological model that is based on optical Bloch equations for a five-level system.

When the excitation energy is decreased the signal traces reveal significantly faster decay rates and the heavy-hole exciton transition is shifted to lower energies. Both experimental results are attributed to an increased captured QW electron density n_e due to higher transparency of the ZnSe buffer layer and reduced Auger escape of QW electrons that leads

to higher exciton-electron scattering rates and an increasing Stark-shift of the X_h exciton transition.

In temperature dependent measurements we observe a filling of the signal dip at $\tau_{12} \approx 0$ and a transition from the PCP effect to a $\chi^{(3)}$ FWM process when the temperature is below 35 K. This behavior is attributed to a reduced mobility of positive charges at the ZnSe/GaAs interface due to localization that lowers the ability to form an electron grating. At temporal pulse overlap $\tau_{12} \approx 0$ the PCP effect is still the dominant process as confirmed by polarization dependent three-pulse experiments. Above 55 K the PCP signal intensity significantly drops which is attributed to an increased mobility of interface holes and thermally activated tunneling of QW electrons back to the GaAs substrate. Two beam FWM experiments where carriers in the GaAs substrate are generated by cw illumination are consistent with the proposed mechanism of the observed PCP effect.

ACKNOWLEDGMENTS

Stimulating discussions with W. Langbein are kindly acknowledged. This work is supported by the National Science Foundation (Grant No. DMR 0305076).

*Present address: Siemens VDO Automotive AG, Siemensstrasse 12, D-93055 Regensburg, Germany

[1] D. D. Nolte, D. H. Olson, G. E. Doran, W. H. Knox, and A. M. Glass, J. Opt. Soc. Am. B **7**, 2217 (1990).
[2] A. Partovi, A. M. Glass, D. H. Olson, G. J. Zydzik, K. T. Short, R. D. Feldmann, and R. F. Austin, Appl. Phys. Lett. **59**, 1832 (1991).
[3] Q. N. Wang, D. D. Nolte, and M. R. Melloch, Appl. Phys. Lett. **59**, 256 (1991).
[4] Q. N. Wang, D. D. Nolte, and M. R. Melloch, J. Appl. Phys. **74**, 4254 (1993).
[5] K. M. Kwolek, M. R. Melloch, and D. D. Nolte, Appl. Phys. Lett. **65**, 385 (1994).
[6] N. T. Pelekanos, B. Devaud, P. Gravey, J. M. Gerard, J. Helbig, and J. Kuhl, Opt. Mater. (Amsterdam, Neth.) **4**, 358 (1995).
[7] N. T. Pelekanos, B. Devaud, C. Guillemot, P. Gravey, J. M. Gerard, B. Lambert, A. Le Corre, and J. E. Viallet, Opt. Mater. (Amsterdam, Neth.) **4**, 348 (1995).
[8] A. Partovi, Opt. Mater. (Amsterdam, Neth.) **4**, 330 (1995).
[9] I. Lahiri, D. D. Nolte, E. S. Harmon, M. R. Melloch, and J. M. Woodall, Appl. Phys. Lett. **66**, 2519 (1995).
[10] K. M. Kwolek, M. R. Melloch, D. D. Nolte, and G. A. Brost, Appl. Phys. Lett. **67**, 736 (1995).
[11] I. Lahiri, K. M. Kwolek, D. D. Nolte, and M. R. Melloch, Appl. Phys. Lett. **67**, 1408 (1995).
[12] I. Lahiri, M. Aguilar, D. D. Nolte, and M. R. Melloch, Appl. Phys. Lett. **68**, 517 (1996).
[13] W. Feng, Z. G. Zhang, Y. Yu, Q. Huang, P. M. Fu, and J. M. Zhou, J. Appl. Phys. **79**, 7404 (1996).
[14] C. De Matos, A. Le Corre, H. L'Haridon, S. Gosselin, and B. Lambert, Appl. Phys. Lett. **70**, 3591 (1997).
[15] A. Le Corre, C. De Matos, H. L'Haridon, S. Gosselin, and B. Lambert, Appl. Phys. Lett. **70**, 1575 (1997).
[16] P. Tayebati, C. Hantzis, and R. N. Sacks, Appl. Phys. Lett. **70**, 691 (1997).
[17] M. H. Zhang, Q. Huang, Y. F. Zhang, J. M. Zhou, Q. Li, and Z. Y. Xu, Appl. Phys. Lett. **75**, 1366 (1999).
[18] S. Iwamoto, H. Kageshima, T. Yuasa, M. Nishioka, T. Someya, Y. Arakawa, F. Fukutani, T. Shimura, and K. Kuroda, J. Appl. Phys. **89**, 5889 (2001).
[19] H. Kageshima, S. Iwamoto, M. Nishioka, T. Someya, K. Fukutani, Y. Arakawa, T. Shimura, and K. Kuroda, Appl. Phys. B: Lasers Opt. **72**, 685 (2001).
[20] A. Partovi, A. M. Glass, T. H. Chui, and D. T. H. Liu, Opt. Lett. **18**, 906 (1993).
[21] Y. Ding, R. M. Brubaker, D. D. Nolte, M. R. Melloch, and A. M. Weiner, Opt. Lett. **22**, 718 (1997).
[22] I. Lahiri, L. J. Pyrak-Nolte, D. D. Nolte, M. R. Melloch, R. A. Kruger, G. D. Bacher, and M. B. Klein, Appl. Phys. Lett. **73**, 1041 (1998).
[23] R. Jones, S. C. W. Hyde, M. J. Lynn, N. P. Barry, J. C. Dainty, P. M. W. French, K. M. Kwolek, D. D. Nolte, and M. R. Melloch, Appl. Phys. Lett. **69**, 1837 (1996).
[24] H. Haas, N. Magnea, J. L. Pautrat, S. Gosselin, T. Baron, and Le Si Dang, Opt. Mater. (Amsterdam, Neth.) **4**, 339 (1995).
[25] D. Lee, J. E. Zucker, R. D. Feldman, and R. F. Austin, Appl. Phys. Lett. **57**, 1132 (1990).
[26] H. P. Wagner, S. Tripathy, H.-P. Tranitz, and W. Langbein, Phys. Rev. Lett. **94**, 147402 (2005).
[27] H. P. Wagner, H.-P. Tranitz, and R. Schuster, Phys. Rev. B **60**, 15 542 (1999).
[28] H. P. Wagner, H.-P. Tranitz, and R. Schuster, Phys. Status Solidi B **221**, 499 (2000).
[29] H. Wang, K. B. Ferrio, D. G. Steel, P. R. Berman, Y. Z. Hu, R. Binder, and S. W. Koch, Phys. Rev. A **49**, R1551 (1994).
[30] M. Wörz, E. Griebl, Th. Reisinger, B. Flierl, D. Haserer, T. Semmler, T. Frey, and W. Gebhardt, Phys. Status Solidi B **202**, 805 (1997).
[31] H. P. Wagner, A. Schätz, R. Maier, W. Langbein, and J. M. Hvam, Phys. Rev. B **57**, 1791 (1998).
[32] H. P. Wagner and S. Tripathy, Phys. Rev. B **69**, 125325 (2004).
[33] H. P. Wagner, A. Schätz, W. Langbein, J. M. Hvam, and Arthur L. Smirl, Phys. Rev. B **60**, 4454 (1999).
[34] H. P. Wagner, S. Tripathy, and P. Bajracharya (unpublished).
[35] L. Schultheis, J. Kuhl, A. Honold, and C. W. Tu, Phys. Rev. Lett. **57**, 1635 (1986).